MICROCOPY RESOLUTION TEST CHART

NATIONAL BUREAU OF STANDARDS

REPORT DOCUMENTATION PAGE		READ INSTRUCTIONS BEFORE COMPLETING FORM
1. REPORT NUMBER NRL Memorandum Report 4823	2. GOVT ACCESSION NO. AD-A114 984	3. RECIPIENT'S CATALOG NUMBER
4. TITLE *(and Subtitle)* NONLINEAR EVOLUTION OF CONVECTING PLASMA ENHANCEMENTS IN THE AURORAL IONOSPHERE II: SMALL SCALE IRREGULARITIES		5. TYPE OF REPORT & PERIOD COVERED Interim report on a continuing NRL problem.
		6. PERFORMING ORG. REPORT NUMBER
7. AUTHOR(s) M. J. Keskinen and S. L. Ossakow		8. CONTRACT OR GRANT NUMBER(s)
9. PERFORMING ORGANIZATION NAME AND ADDRESS Naval Research Laboratory Washington, D.C. 20375		10. PROGRAM ELEMENT, PROJECT, TASK AREA & WORK UNIT NUMBERS 62715H; RR0330244; 47-0883-0-2, 47-0889-0-2
11. CONTROLLING OFFICE NAME AND ADDRESS Defense Nuclear Agency, Washington, D.C. 20305 Office of Naval Research, Arlington, VA. 22217		12. REPORT DATE May 18, 1982
		13. NUMBER OF PAGES 33
14. MONITORING AGENCY NAME & ADDRESS(*if different from Controlling Office*)		15. SECURITY CLASS. *(of this report)* UNCLASSIFIED
		15a. DECLASSIFICATION/DOWNGRADING SCHEDULE

16. DISTRIBUTION STATEMENT *(of this Report)*

Approved for public release; distribution unlimited.

17. DISTRIBUTION STATEMENT *(of the abstract entered in Block 20, if different from Report)*

19. KEY WORDS *(Continue on reverse side if necessary and identify by block number)*

Plasma convection   Irregularities
Gradient-drift instability   Aurora

20. ABSTRACT *(Continue on reverse side if necessary and identify by block number)*

The linear stability and nonlinear evolution of small scale ($\sim$ 0.1-1 km) density irregularities in local unstable regions of large scale convecting auroral plasma enhancements have been studied using analytical and numerical simulation techniques. Our results show that these small scale size irregularities are driven unstable primarily by the effects of convection and field aligned currents. Furthermore, we find that the density irregularities, in the nonlinear regime, in a plane nearly perpendicular to the magnetic field, resemble steepened striation-like structures (elongated in the

(Continues)

DD FORM 1473 EDITION OF 1 NOV 65 IS OBSOLETE
1 JAN 73
S/N 0102-014-6601

20. ABSTRACT (Continued)

north-south direction for equatorward convection) which can form and cascade from kilometer to tens of meter scale sizes on the order of an hour. The one-dimensional spatial power spectra of the density irregularities in the north-south $P(k_y) \propto k_y^{-n}$ and east-west $P(k_x) \propto k_x^{-n}$ can be described by inverse power laws with $n \simeq$ 2-3. Finally, we propose and demonstrate, using a crude model, that a two-step process, in which small scale irregularities can grow on longer wavelength nonlinear structures, can account for the experimentally observed L-shell aligned nature of the irregularities.

CONTENTS

NONLINEAR EVOLUTION OF CONVECTING PLASMA ENHANCEMENTS IN THE AURORAL IONOSPHERE II: SMALL SCALE IRREGULARITIES

1. INTRODUCTION

Using both radar and satellite measurements, large scale convecting plasma enhancements in the auroral ionosphere have recently been identified and studied [Vickrey et al., 1980]. Observed in regions of diffuse auroral particle precipitation and associated field-aligned currents, these enhancements have overall latitudinal dimensions of a few hundred kilometers, contain relatively steep poleward and equatorward edges, and have been shown to be approximately field-aligned resembling vertical slabs of ionization. Their occurrence, which is maximized in the evening-midnight sector, is apparently not strongly related to magnetic activity nor to E-region processes. The presence of plasma density irregularities associated with these enhancements has been verified using satellite scintillation studies [Fremouw et al. 1977; Rino et al., 1978; Vickrey et al., 1980]. The scintillation data have indicated that the electron density irregularities are structured like L-shell aligned sheets [Fremouw et al., 1977; Rino et al., 1978]. In addition, Rino and Matthews [1980] have shown that the scintillation enhancements resulting from these irregularities cannnot be explained in terms of a geometrical enhancement alone. A purely geometrical enhancement occurs when the signal propagation path intercepts an axis transverse to the magnetic field along which axis the irregularities have a high degree of spatial coherence. Moreover, the source region of these scintillation causing irregularities has been demonstrated to be latitude limited [Rino and Owen, 1980] and contained in a vertical slab of F region plasma. Using simultaneous rocket probe, scintillation and incoherent scatter, Kelley et al. [1980] have also recently studied several characteristics of auroral F region irregularities, e.g., total electron content and spatial power spectra.

Since these ionization enhancements have been observed while convecting equatorward, their poleward edges could be unstable to the $\underline{E} \times \underline{B}$ gradient drift instability [Simon, 1963; Linson and Workman, 1970] as observed in artificial ionospheric plasma clouds. Indeed, for observed [Vickrey et al., 1980] plasma enhancement density gradient scale lengths of $L \approx 10\text{-}50$ km and convection velocities of approximately 200 m/sec ($E_o \approx 10$ mV/m) reasonable

growth rates for the $\underline{E} \times \underline{B}$ gradient drift instability can be expected since $\gamma^{-1} \simeq (BL/cE_o) \approx 50-250$ sec where γ is the $\underline{E} \times \underline{B}$ growth rate, B is the ambient magnetic field and c is the speed of light. Moreover, it has been shown [Ossakow and Chaturvedi, 1979] that by applying the current convective instability [Lehnert, 1958; Kadomtsev and Nedospasov, 1960] the equatorward side of the plasma enhancements, which is stable to the $\underline{E} \times \underline{B}$ gradient drift instability, can be driven unstable by the ambient field aligned particle precipitation currents in conjunction with the equatorward density gradients. Other mechanisms that might account for these irregularities are structured low energy particle precipitation [Kelley et al., 1980, 1982] and irregular field aligned currents. Keskinen et al. [1980] showed that the nonlinear state of the large scale irregularities in the equatorward edges of these plasma enhancements could be characterized by poleward convecting plasma depletions and equatorward-moving enhancements. In addition, they demonstrated that these irregularities could be described by inverse power laws in the nonlinear regime. Recently, Keskinen and Ossakow [1982] discussed the linear stability and nonlinear evolution of large scale convecting plasma enhancements in arbitrary ambient electric fields in the auroral ionosphere. These studies showed that convection (through the $\underline{E} \times \underline{B}$ gradient drift instability) is the primary driver of long wavelength (3-100 km) irregularities in diffuse auroral F region plasma enhancements. However, the aforementioned satellite scintillation measurements [Rino et al., 1978] have indicated that the density irregularities associated with the plasma enhancements have scale sizes down to hundreds of meters. It is of interest to study these small scale ($\sim 0.1-1$ km) irregularities in order to compare with and supplement experimental observations.

In this report we present a linear analytical and nonlinear numerical study of small scale irregularities applicable to local unstable regions of large scale convecting auroral plasma enhancements. In Section 2 we give a linear stability analysis of the plasma fluid equations which describe the evolution of density fluctuations in the auroral F region ionospheric plasma. In Section 3 we outline the methods used to numerically solve these equations, while in Section 4 our principal results are given. Finally, in Section 5 we summarize and discuss our findings.

2. EQUATIONS OF MOTION AND LINEAR THEORY

For wavelengths greater than the ion mean free path we use fluid equations to describe the ion and electron plasma. The following geometry is used: the y-axis is in the north-south direction, the x-axis points west, and the z-axis is downward along the magnetic field. In this report we ignore the vertical density gradient which is weaker than the horizontal plasma density gradients [Vickrey et al., 1980] in the typical diffuse auroral plasma enhancements. The ion and electron fluids then obey the following equations

$$\frac{\partial n}{\partial t} + \nabla \cdot (n \; \underline{v}_e) = 0 \tag{1}$$

$$\frac{\partial n}{\partial t} + \nabla \cdot (n \; \underline{v}_i) = 0 \tag{2}$$

$$\underline{v}_e = \frac{cT_e}{B} \frac{\nabla_\perp n \times \hat{z}}{n} + \frac{cE_\perp \times \hat{z}}{B} - \frac{\nu_{ei} c_s^2}{\Omega_e \Omega_i} \frac{\nabla_\perp n}{n} - \frac{eE_z}{m\nu_{ei}}$$

$$- \left(\frac{T_e}{m\nu_{ei}} + \frac{c_s^2}{\nu_{in}} \right) \frac{1}{n} \frac{\partial n}{\partial z} \hat{\underline{z}} + v_o \hat{\underline{z}} \tag{3}$$

$$\underline{v}_i = \frac{cE_\perp \times \hat{z}}{B} + \frac{\nu_{in}}{\Omega_i} \frac{cE_\perp}{B} - \frac{cT_i}{eB} \frac{\nabla_\perp n \times \hat{z}}{n} - \frac{\nu_{in} cT_i}{\Omega_i eB} \frac{\nabla_\perp n}{n}$$

$$- \frac{\nu_{ei}}{\Omega_e} \frac{c_s^2}{\Omega_i} \frac{\nabla_\perp n}{n} - \frac{c_s^2}{\nu_{in}} \frac{1}{n} \frac{\partial n}{\partial z} \hat{\underline{z}} + V_o \hat{\underline{z}} \tag{4}$$

$$\nabla \cdot \underline{J} = 0 \tag{5}$$

Here n_σ ($\sigma = i$ or e) is the species density and $\underline{E}$ is the total electric field. Since we will be interested in low frequency fluctuations we have ignored inertial terms in the electron and ion momentum equations (3) and (4). Equation (5) results from the assumption of quasineutral

3

fluctuations $n_e \simeq n_i \equiv n$. In addition, v_o and V_o refer to the electron and ion velocities along the magnetic field giving rise to the diffuse auroral current. The symbol ν_{in} denotes the ion-neutral collision frequency, ν_{ei} the electron-collision frequency, c the speed of light, $T_e \simeq T_i \equiv T$ the species temperature, c_s the ion acoustic speed and $\Omega_i (\Omega_e)$ the ion (electron) gyro-frequency. We have neglected ν_{en} compared with ν_{ei} and taken $v_\sigma / \Omega_\sigma \ll 1$ for $\sigma = i,e$ (F region approximation).

Any two of equations (1), (2), and (5) provide a complete description of the problem. We will use the ion continuity equation (1) and (5). After separating the total electric field into an ambient and fluctuating part $\underline{E}_\perp = \underline{E}_o - \nabla_\perp \delta\phi$ and transforming to a frame drifting with velocity $\underline{V}_o = -(c/B) [\hat{\underline{z}} \times \underline{E}_o - (\nu_{in}/\Omega_i) \underline{E}_o]$ we can write

$$\frac{\partial n}{\partial t} + \frac{c}{B} \left[\hat{z} \times \nabla_\perp \delta\phi \cdot \nabla_\perp n - (\nu_{in}/\Omega_i) \nabla_\perp \delta\phi \cdot \nabla_\perp n \right] =$$

$$\left(\frac{\nu_{in}}{\Omega_i} \frac{cT_i}{eB} + \frac{\nu_{ei}}{\Omega_e} \frac{c_s^2}{\Omega_i} \right) \nabla_\perp^2 n + \frac{c_s^2}{\nu_{in}} \frac{\partial^2 n}{\partial z^2} \tag{6}$$

$$\nabla_\perp \cdot (n \nabla_\perp \delta\phi) + \frac{\Omega_i \Omega_e}{\nu_{in} \nu_{ei}} \frac{\partial}{\partial z} \left(n \frac{\partial \delta\phi}{\partial z} \right) = \left(\underline{E}_o - \frac{\Omega_i}{\nu_i} \frac{B}{c} \underline{V}_d \right) \cdot \nabla n$$

$$- \frac{T}{e} \left(\nabla_\perp^2 n - \frac{\Omega_i \Omega_e}{\nu_{in} \nu_{ei}} \frac{\partial^2 n}{\partial z^2} \right) \tag{7}$$

where $\underline{V}_d = \hat{\underline{z}} (v_o - V_o)$. Linearizing (6) and (7) by separating $n = n_o(y) + \delta n$ with δn, $\delta\phi \propto \exp[i(k_x x + k_z z - \omega t)]$, $\omega = \omega_r + i\gamma$, $kL \gg 1$, $L^{-1} \equiv (1/n_o)(\partial n_o/\partial y)$ we find a growth rate ($k_\parallel \equiv k_z$)

$$\gamma = \frac{-\dfrac{\nu_{ei}}{\Omega_e} \dfrac{1}{L} \left(\dfrac{\nu_{in}}{\Omega_i} \dfrac{cE_o}{B} - \theta V_d \right)}{\theta^2 + \dfrac{\nu_{in}}{\Omega_i} \dfrac{\nu_{ei}}{\Omega_e}} - D_\perp k_x^2 - D_\parallel k_z^2 \tag{8}$$

4

where $\theta \equiv k_z/k_x$, $\underline{E}_o \equiv E_o\hat{x}$, and $D_\perp = (\nu_{ei}/\Omega_e\Omega_i)c_s{}^2$ and $D_\parallel = (c_s{}^2/\nu_{in})\{1 + [(\nu_{in}/\Omega_i)^2/((\nu_{ei}\nu_{in}/\Omega_e\Omega_i) + (k_z{}^2/k_\perp{}^2))]\}$. The general expression for the instability growth rate γ using arbitrary directions of $\underline{k}$ and $\underline{E}_o$ can be found in <u>Keskinen and Ossakow</u> [1982]. In regions of plasma enhancements where $\partial n_o/\partial y < 0$ ($L < 0$) we find the condition for unstable growth to be

$$[(\nu_{in}/\Omega_i)(cE_{ox}/B) + |V_d|] > \frac{\Omega_e|L|}{\nu_{ei}}\left[\theta^2 + \frac{\nu_{in}}{\Omega_i}\frac{\nu_{ei}}{\Omega_e}\right]\left[D_\perp k_x^2\left(1 + \frac{D_\parallel}{D_\perp}\theta^2\right)\right]$$

where we have taken, for example, the currents to be downward, i.e., $V_d < 0$. The effects of the field-aligned currents will be able to reduce ($\theta < 0$) or enhance ($\theta > 0$) the $\underline{E} \times \underline{B}$ gradient drift instability growth rate. However, when $\partial n_o/\partial y > 0$ ($L > 0$) the condition for unstable growth can be satisfied for large enough current velocities

$$|V_d| > (\nu_{in}/\Omega_i)(cE_{ox}/B|\theta|) + \frac{\Omega_e|L|}{\nu_{ei}|\theta|}\left[\theta^2 + \frac{\nu_{in}}{\Omega_i}\frac{\nu_{ei}}{\Omega_e}\right]\left[D_\perp k_x^2\left(1 + \frac{D_\parallel}{D_\perp}\theta^2\right)\right].$$

The expression for the growth rate γ in equation (8) can be maximized as a function of $\theta = k_\parallel/k_x$, a measure of field-alignment, using $\partial\gamma/\partial\theta|_{\theta=\theta_m} = 0$ giving

$$\theta_m = \frac{\nu_{in}}{\Omega_i}\frac{cE_{ox}}{B V_d}\quad\left[\left(\frac{cE_{ox}}{B V_d}\right)^2\left(\frac{\nu_{in}}{\Omega_i}\right)^2 + \left(\frac{\nu_{ei}\nu_{in}}{\Omega_e\Omega_i}\right)\right]\tag{9}$$

Using typical diffuse auroral F region parameters $\nu_{in}/\Omega_i \simeq 10^{-4}$, $\nu_{ei}/\Omega_e \simeq 10^{-4}$, $E_{ox} \simeq 10$ mV/m, $j_\parallel = n_o eV_d \simeq 1$ μA/m^2, $B = 0.5$G, $n_o \simeq 10^5$cm^{-3} this gives $|\theta_m| \simeq 10^{-4}$, i.e., approximate field alignment. Inserting these parameters into eq. (8) with $L \simeq 20$ km, $D_\perp \simeq 0.2$ m^2/sec and $D_\parallel \simeq 10^8$m^2/sec we find that the fastest growing linear modes have growth times $\gamma_{max}^{-1} \simeq 10^2$ sec.

5

3. NONLINEAR THEORY

In order to study the nonlinear evolution of these small scale irregularities, we must resort to a numerical solution of the nonlinear set of equations (6) and (7) due to their complex nature. Equations (6) and (7) can be written in dimensionless form by introducing the following scaled quantities $\hat{n} = n_o/N_o$, $\hat{\delta\phi} = \delta\phi/BL$, $\hat{x} = x/L$, $\hat{y} = y/L$, $\hat{z} = z/L$, $\hat{t} = ct/L$ as follows (where we have dropped the tilde for clarity)

$$\frac{\partial n}{\partial t} + \frac{\partial \delta\phi}{\partial x}\frac{\partial n}{\partial y} - \frac{\partial \delta\phi}{\partial y}\frac{\partial n}{\partial x} - c_1\left(\frac{\partial \delta\phi}{\partial x}\frac{\partial n}{\partial x} + \frac{\partial \delta\phi}{\partial y}\frac{\partial n}{\partial y}\right) = c_2\left(\frac{\partial^2 n}{\partial x^2} + \frac{\partial^2 n}{\partial y^2}\right) + c_3\frac{\partial^2 n}{\partial z^2}$$

(10)

$$\frac{\partial^2 \delta\phi}{\partial x^2} + \frac{\partial^2 \delta\phi}{\partial y^2} + \frac{1}{n}\left(\frac{\partial n}{\partial y}\frac{\partial \delta\phi}{\partial y} + \frac{\partial n}{\partial x}\frac{\partial \delta\phi}{\partial x}\right) + c_4\left(\frac{\partial^2 \delta\phi}{\partial z^2} + \frac{1}{n}\frac{\partial n}{\partial z}\frac{\partial \delta\phi}{\partial z}\right)$$

$$= c_5\frac{\partial n}{\partial x} + c_6\frac{\partial n}{\partial y} - c_7\frac{\partial n}{\partial z} - c_8\frac{1}{n}\left(\frac{\partial^2 n}{\partial x^2} + \frac{\partial^2 n}{\partial y^2}\right) + c_9\frac{1}{n}\frac{\partial^2 n}{\partial z^2}$$

(11)

with c_i, $i = 1, \ldots, 9$ dimensionless constants given by $c_1 = \nu_{in}/\Omega_i$, $c_2 = (\nu_{in}/\Omega_i)(T_i/eBL) + (\nu_{ei}/\Omega_e)(c_s^2/\Omega_i cL)$, $c_3 = c_s^2/\nu_{in}cL$, $c_4 = \Omega_e\Omega_i/\nu_e\nu_i$, $c_5 = E_{ox}/B$, $c_6 = E_{oy}/B$, $c_7 = (\Omega_i/\nu_i)(V_d/c)$, $c_8 = T/eBL$, $c_9 = (\Omega_e\Omega_i/\nu_e\nu_i)\ c_8$.

In the following numerical simulations we take advantage of the fact that the fastest growing, most dangerous modes from linear theory are almost field-aligned, i.e., $k_\parallel/k_\perp \ll 1$ where $k_\parallel(k_\perp)$ is the component of $\underline{k}$ parallel (perpendicular) to the magnetic field. These waves are of most interest to us and, as a result, we solve equations (10) and (11) in a plane containing these modes which is nearly perpendicular to the magnetic field while fixing the value of $k_\parallel/k_x \ll 1$. A similar approach has been adopted in numerical studies of drift-wave [Lee and Okuda, 1976] and trapped-particle [Matsuda and Okuda, 1976] instabilities in laboratory plasmas. The system of equations (10) and (11) was first transformed to the x'y'z' coordinate system (as shown in Fig. 1) by a simple rotation about the y-axis by the angle $\theta = k_\parallel/k_x \ll 1$ using
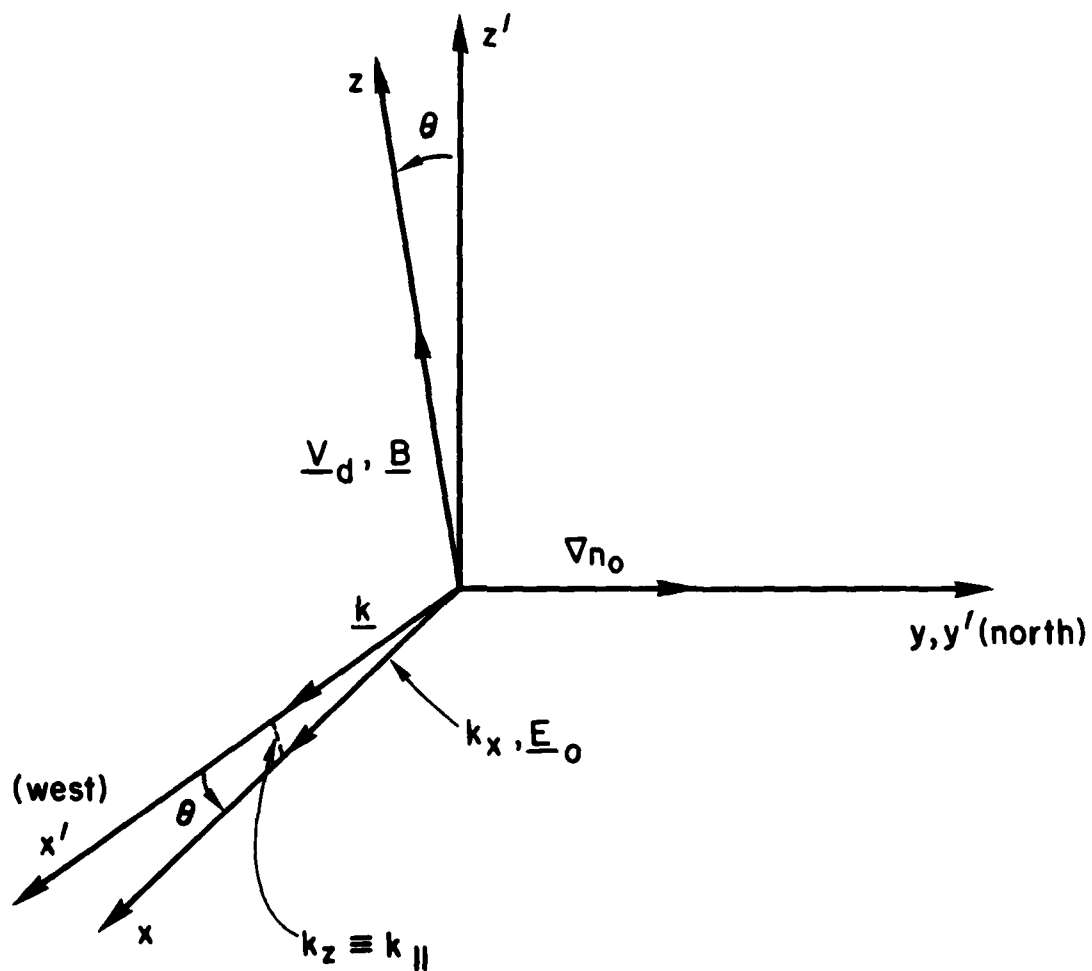
6

Fig. 1 - Coordinate system used in simulations. The x´y´ is the simulation plane. The x´,x,z´,z axes are coplanar.

7

$$\frac{\partial}{\partial x} = \cos \theta \frac{\partial}{\partial x'} - \sin \theta \frac{\partial}{\partial z'}$$

$$\frac{\partial}{\partial z} = \sin \theta \frac{\partial}{\partial x'} + \cos \theta \frac{\partial}{\partial z'}$$

$$\frac{\partial}{\partial y} = \frac{\partial}{\partial y'}$$

where θ is the angle for maximum linear growth rate defined by eq. (12) for a definite set of parameters ν_{in}/Ω_i, cE_{ox}/BV_d, ν_{ei}/Ω_e. Since $\theta \ll 1$ this transformation can be written $\partial/\partial x \simeq \partial/\partial x'$, $\partial/\partial z \simeq \theta \partial/\partial x'$, $\partial/\partial y = \partial/\partial y'$ with $\partial/\partial z' = 0$. As a consequence the three dimensional problem is reduced to two-dimensions. By solving equations (10) and (11) in the $x'y'z'$ coordinate system a small but finite $k_\parallel$ is effectively introduced into the model.

Equations (10) and (11) were then solved numerically on a mesh consisting of 64 grid points in the north-south direction (y-direction) and 64 grid points in the east-west direction (x-direction) with constant grid spacing of 15 m. As a result, the simulation plane, which is taken to be essentially horizontal at an altitude of 350 km in the diffuse auroral F region, has a north-south and east-west extent of 960 m, respectively. The field aligned currents are taken to be constant in space and time over the grid. The plasma density n in equation (10) was advanced in time using a multi-dimensional flux-corrected variable timestep leapfrog-trapezoid scheme [Zalesak, 1979] which is second order in time and fourth order in space. At each timestep the self-consistent electrostatic potential $\delta\phi$ of the plasma enhancement in eq. (11) was determined using a Chebychev iterative method [McDonald, 1980] with a convergence criterion of 10^{-4}. Since we are considering a small local unstable region (960 m by 960 m) of a large scale plasma enhancement which is several hundred kilometers in extent, periodic boundary conditions were imposed both in the east-west and north-south directions.

4. RESULTS

In the following we consider the linear and nonlinear evolution of small scale irregularities in plasma enhancements in the diffuse auroral F region ionosphere in an approximately horizontal plane at 350 km altitude almost

8

perpendicular to the magnetic field. We take the following typical parameters [Vickrey et al., 1980; Schunk and Walker, 1973; Banks and Kockarts, 1973] L = 20 km, $\nu_{in}/\Omega_i = 2 \times 10^{-4}$, $\nu_{ei}/\Omega_e = 2 \times 10^{-4}$, $E_{ox} = 10$ mV/m $T_e = T_i = 1000^{\circ}$K and $J_{\parallel} = 1$ μA/m^2 (which gives a current velocity of $V_d \simeq 60$ m/sec with $N_o \simeq 1 \times 10^5$cm^{-3}). In addition, we assume that the diffuse auroral particle precipitation current $J_{\parallel}$ is downward ($V_d < 0$) and spatially and temporally uniform over the entire plasma enhancement. In order to find the location and magnitude of the maximum linear growth rates to be expected with this set of parameters we first compute $\theta_m = k_{\parallel}/k_x$ as given in eq. (9) with $V_d \equiv - |V_d| = - 60$ m/sec. This gives two values for θ_m which are $\theta^+ = 1.4 \times 10^{-5}$ and $\theta^- = - 6.5 \times 10^{-4}$. Using eq. (9) and considering wavelengths $\lambda_x \equiv 2\pi/k_x = 500$ m the first value θ^+ gives a maximum linear growth rate $\gamma_{max} \simeq 1.0 \times 10^{-2}$sec^{-1} on the poleward side ($\partial n_o/\partial y < 0$) with linearly damped perturbations $\gamma_{max} \simeq -3.5 \times 10^{-3}$sec^{-1} on the equatorward side ($\partial n_o/\partial y > 0$). The second value θ^- gives only a marginally unstable growth rate of $\gamma_{max} \simeq 8 \times 10^{-5}$sec^{-1} on the equatorward side with damped fluctuations $\gamma_{max} \simeq -3.7 \times 10^{-4}$sec^{-1} on the poleward side. These results agree with the experimental observations [Vickrey et al., 1980] that the largest linear growth rates occur on the poleward side of the equatorward convecting plasma enhancements. In this case the effect of the field-aligned currents is to enhance the $\underline{E} \times \underline{B}$ gradient-drift instability growth rate on the poleward side. The current velocities are too weak for the cases studied observationally to give appreciable growth on the equatorward side of the plasma enhancements. We will then consider the evolution of modes satisfying $\theta^+ = k_{\parallel}/k_x = 1.4 \times 10^{-5}$.

A slab approximation, with initial density profile $n_o(y') = N_o[1 - y'/L + \epsilon(x',y')]$, $N_o = 10^5$cm^{-3}, is used to model a small local unstable region on the poleward side of a zero order equatorward convecting large scale plasma enhancement in the diffuse auroral F region ionosphere. In this assumed profile, $\epsilon(x',y')$ denotes the initial perturbation and L = 20, 30 km the initial plasma enhancement density gradient scale length. We consider two models distinguished by the initial seed perturbations $\epsilon(x',y')$. In Model 1, purely random white noise-like initial conditions are used with $\epsilon(x',y')$ having a root mean square value of 0.01. In Model 2, a two-dimensional monochromatic perturbation is employed. For Models 1 and 2 we take $E_{ox} = 10$ mV/m, $E_{oy} = 0$. We now drop the prime notation for clarity.

9

Figures 2(a)-2(c) give the evolution of the isodensity contour plot of small scale density fluctuations $\delta n(x,y)/n_o$ using Model 1 with L = 20 km. Figure 2(a) shows the purely random nature of the initial conditions still persists at t = 100 sec. Figure 2(b) gives the evolution of $\delta n/n_o$ at t = 800 sec where some north-south elongation and steepening have occurred. Note that local density enhancements ($\delta n/n_o > 0$, solid contours) are convecting northward (poleward) while local depletions ($\delta n/n_o < 0$, dashed contours) are convected southward (equatorward). This relative movement of enhancements and depletions is directly analogous to the classical Rayleigh-Taylor instability in a heavy fluid supported by a lighter fluid. Doppler radar backscatter signatures [Hanuise et al., 1981] of 10.5 m irregularities in the evening-midnight auroral F region ionosphere also indicate a similar convection pattern in a plane nearly perpendicular to he magnetic field. In this experiments southward irregularity convection was observed approximately 1000 km due north from northward looking HF radar while farther north at a range of 1200 km the irregularities appear convecting northward. Finally, Fig. 2(c) details the density fluctuations in the nonlinear regime at t = 1000 sec. Further elongation and steepening is evident. Similar density contour development was also observed for the other plasma enhancement density gradient scale length used, L = 30 km.

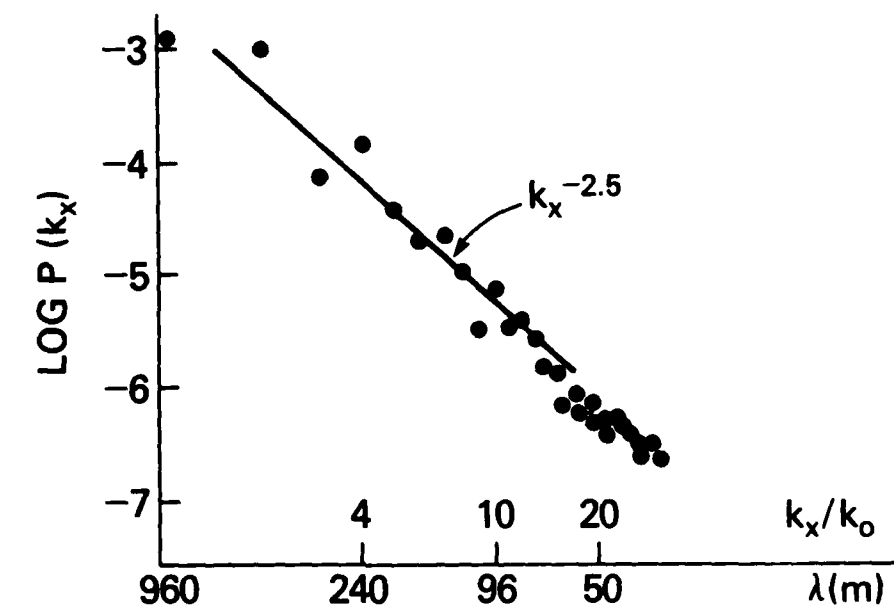Figure 3a-b give sample one-dimensional spatial power spectra in the nonlinear regime at t = 1000 sec both in the east-west ($P(k_x)$) and north-south ($P(k_y)$) directions, respectively for Model 1. These power spectra are defined as follows
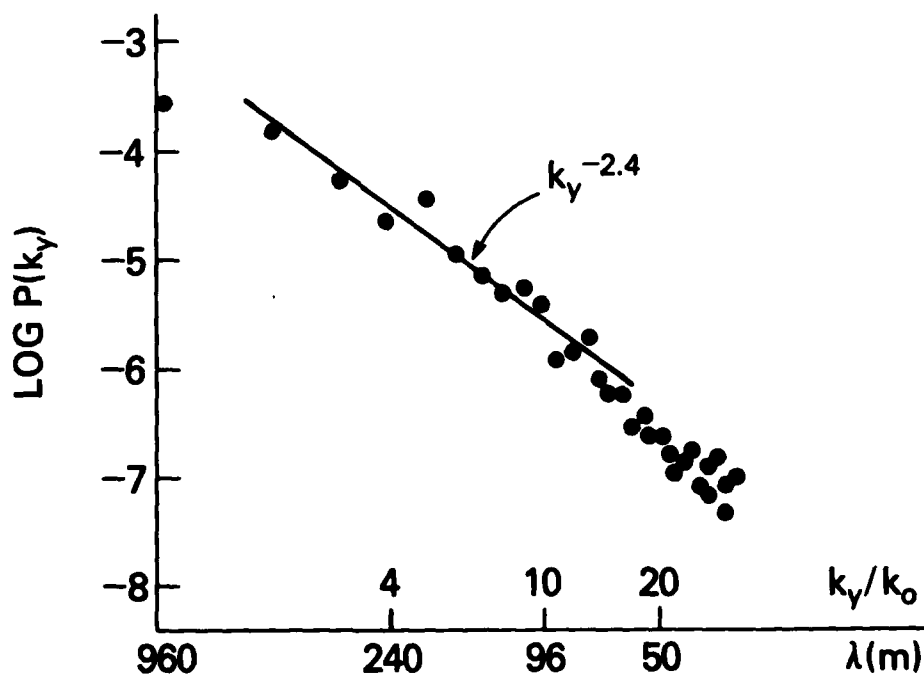
$$P(k_x) = \int dk_y \bar{P}(k_x,k_y)$$

and

$$P(k_y) = \int dk_x \bar{P}(k_x,k_y)$$

where $\bar{P}(k_x,k_y) \equiv (L_x L_y)^{-1}[\delta n(k_x,k_y)/N_o]^2$ is the spectral density, $\delta n = n - N_o$ with n_o the peak plasma enhancement density, and $L_x L_y$ is the area of the numerical simulation plane. For both cases these power spectra are well-fitted with inverse power laws $P(k_x) \approx k_x^{-n}$ and $P(k_y) \approx k_y^{-n}$ with index $n \approx 2-3$. The spectral indices are in agreement with those obtained from

10

Fig. 2 - Isodensity contours of $\delta n/n_o$ with L = 20 km at (a) t = 100 sec, (b) t = 800 sec, (c) t = 1000 sec Model 1. Solid contours denote local enhancements $\delta n/n_o > 0$; dashed contours denote local depletions $\delta n/n_o < 0$. The observer is looking upward along the magnetic field lines.

11

Fig. 3 - One dimensional (a) east-west $P(k_x)$ and (b) north-south $P(k_y)$ spatial power spectra for Model 1 at t = 1000 sec. The solid line is best fit to numerical simulation results (solid circles). The units of $P(k_x)$ and $P(k_y)$ are km with $k_o = 2\pi/960$ m the fundamental wave number.

recent scintillation studies [Erukhimov et al., 1981] of small
scale ($\lesssim$ 1 km) plasma turbulence in the auroral ionosphere.

Figures 4(a)-4(c) illustrate the evolution of the density fluctuations
$\delta n/n_o$ for Model 2 with L = 20 km. The simulations were initialized with a
general monochromatic two-dimensional perturbation of the form [Rognlien and
Weinstock, 1974; Chaturvedi and Ossakow, 1979]

$$\delta n(x,y)/n_o = A_{1,1}\sin k_y y \cos k_x x + A_{2,0}\sin 2 k_y y$$

with $k_x = k_y = 2\pi/960$ m, $A_{1,1} = 2 \times 10^{-4}$, $A_{2,0} = 2 \times 10^{-5}$ where
$A_{1,1}(A_{2,0})$ is linearly unstable (damped). Figure 4(a) gives an isodensity
contour plot of $\delta n(x,y)/n_o$ at t = 0 sec. The initial perturbation describes a
sequence of local enhancements ($\delta n/n_o > 0$) and depletions ($\delta n/n_o < 0$)
arranged in a checkerboard fashion. Figure 4(b) shows the evolution of $\delta n/n_o$
at t = 900 sec where elongation and steepening are again seen. Figure 4(c)
gives $\delta n/n_o$ at t = 1200 sec in the nonlinear regime where further steepening
and north-south elongation can be observed. As in the Model 1 the late time
evolution of the small scale plasma density irregularities on the poleward
side of large-scale equatorward convecting plasma enhancements can be
characterized by poleward moving steepened local enhancements and equatorward
convecting depletions. Spatial power spectra in the nonlinear regime similar
to Model 1 were also observed in Model 2.

However, satellite scintillation studies [Fremouw et al., 1977; Rino et
al., 1978; Rino and Matthews, 1980] dealing with equatorward convecting large-
scale plasma enhancements have indicated that density irregularities with
scale sizes (0.1-1 km) are primarily L-shell (east-west) aligned, i.e., have a
higher degree of spatial coherence along L-shells than in the north-south
direction. On the contrary, the present and a previous study [Keskinen and
Ossakow, 1982] have shown that density irregularities in both the long (1-100
km) and short (0.1-1 km) wavelength regime in equatorward convecting auroral
plasma enhancements are primarily north-south aligned which is consistent with
the nonlinear development of the Rayleigh-Taylor-like $\underline{E} \times \underline{B}$ gradient drift
instability. As shown in Model 2, nonlinear mode coupling effects [Chaturvedi
and Ossakow, 1979] do not appear to be sufficient to account for the L-shell
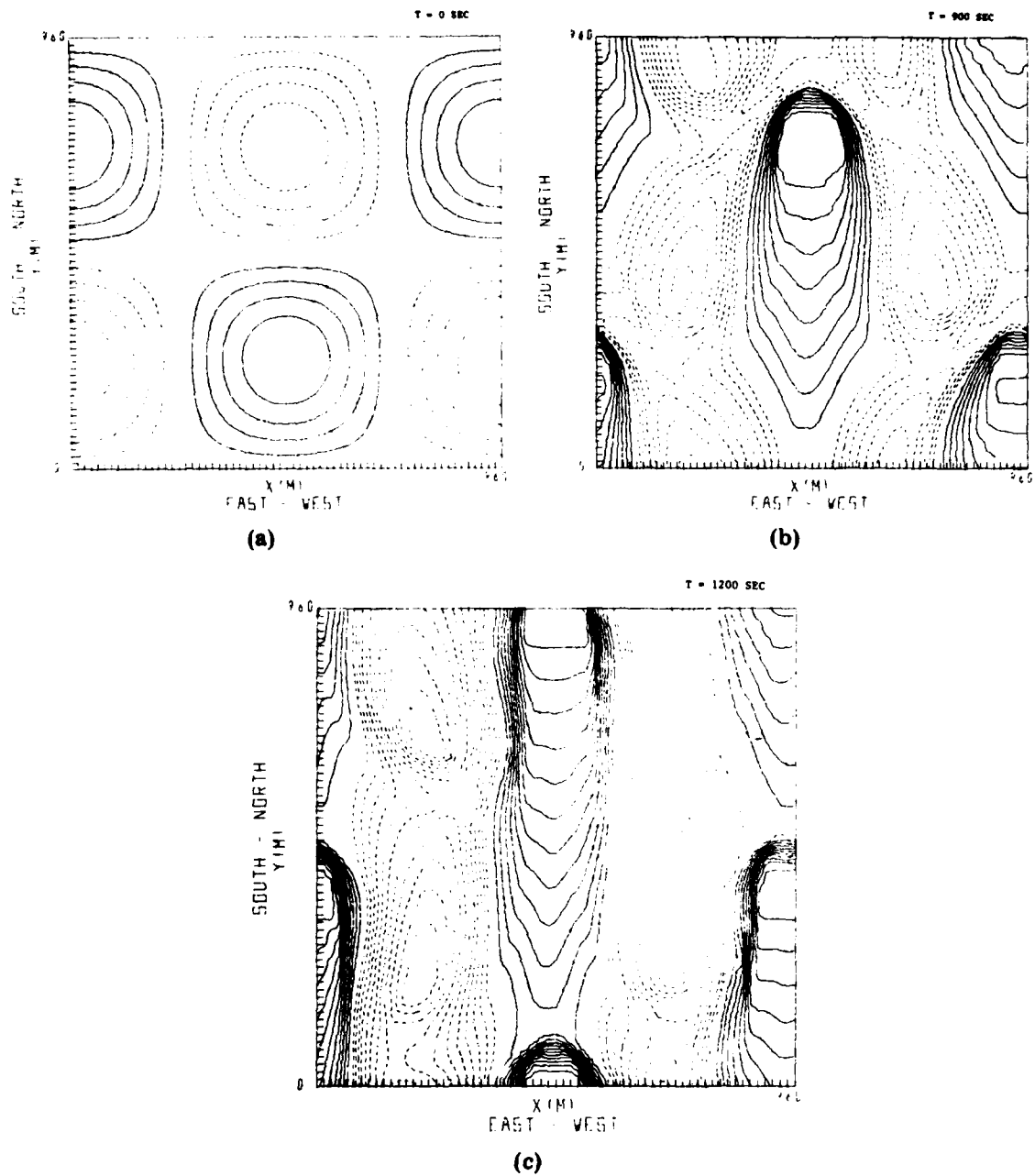alignment. Keskinen and Ossakow [1982] have studied the nonlinear evolution

13

T = 0 SEC

(a)

T = 900 SEC

(b)

T = 1200 SEC

(c)

Fig. 4 — Isodensity contours of $\delta n/n_o$ for L = 20 km at (a) t = 0 sec, (b) t = 900 sec, (c) t = 1200 sec for Model 2 using monochromatic initial conditions.

14

of equatorward convecting plasma enhancements which initially contain only a north-south density gradient. The east-west density gradient in the plasma enhancements is very weak [J. Vickrey, private communication]. These plasma enhancements were shown to be unstable and to break up into primary north-south aligned finger-like structures which themselves contain sharp east-west and north-south density gradients. If these long wavelength primary irregularities have a component of convection in the east-west direction (from a north-south electric field), then secondary smaller scale approximately L-shell aligned structures could grow on the east-west density gradients of the primary irregularities. A north-south electric field is usually present in the evening diffuse auroral F region ionosphere [Banks and Doupnik, 1975; Vickrey et al., 1980]. (Some evidence that this process can occur was presented in Keskinen and Ossakow [1982].) However, the east-west convection must be of sufficient magnitude compared with the north-south convection to prevent velocity shear stabilization [Perkins and Doles, 1975] of the smaller scale secondary irregularities. For an initial density variation along the y-direction with scale length L, the approximate stability criterion is $E_{oy}/E_{ox} > 2/kL$ where k is the perturbation wavenumber and $E_{oy}(E_{ox})$ the component of the $\underline{E} \times \underline{B}$ convective electric field parallel (perpendicular) to the initial density gradient.

Figures 5(a)-5(c) illustrate the evolution of the density fluctuations $\delta n(x,y)/n_o$ for the above secondary, two-step model in which smaller scale size irregularities can grow on larger striation-like structures. We assume that the large scale structures are in the nonlinear regime [Keskinen and Ossakow, 1982] and evolve on a slower time scale than the smaller scale size irregularities. The initial density profile which describes the east-west density gradient of a small local region of a large primary striation is taken, for simplicity, to be of the approximate form $n_o(x) = N_o[1 - x/L + \epsilon(x,y)]$ with $L = 5$ km and $\epsilon(x,y)$ derived from white-noise random initial conditions. For simplicity, we take the total electric field to be northward $(\underline{E}_o \equiv E_o\hat{y})$ of magnitude $|\underline{E}_o| = 10$ mV/m. All other parameters remain the same. Figure 5(a) shows the evolution of the isodensity contour plot at $t = 100$ sec. Figure 5(b) gives $\delta n/n_o$ at $t = 325$ sec where some steepening and elongation in the east-west direction (L-shell alignment) has occurred. Finally, Fig. 5(c), which shows further steepening at $t = 400$ sec in the nonlinear regime, clearly illustrates L-shell aligned structures. The spatial
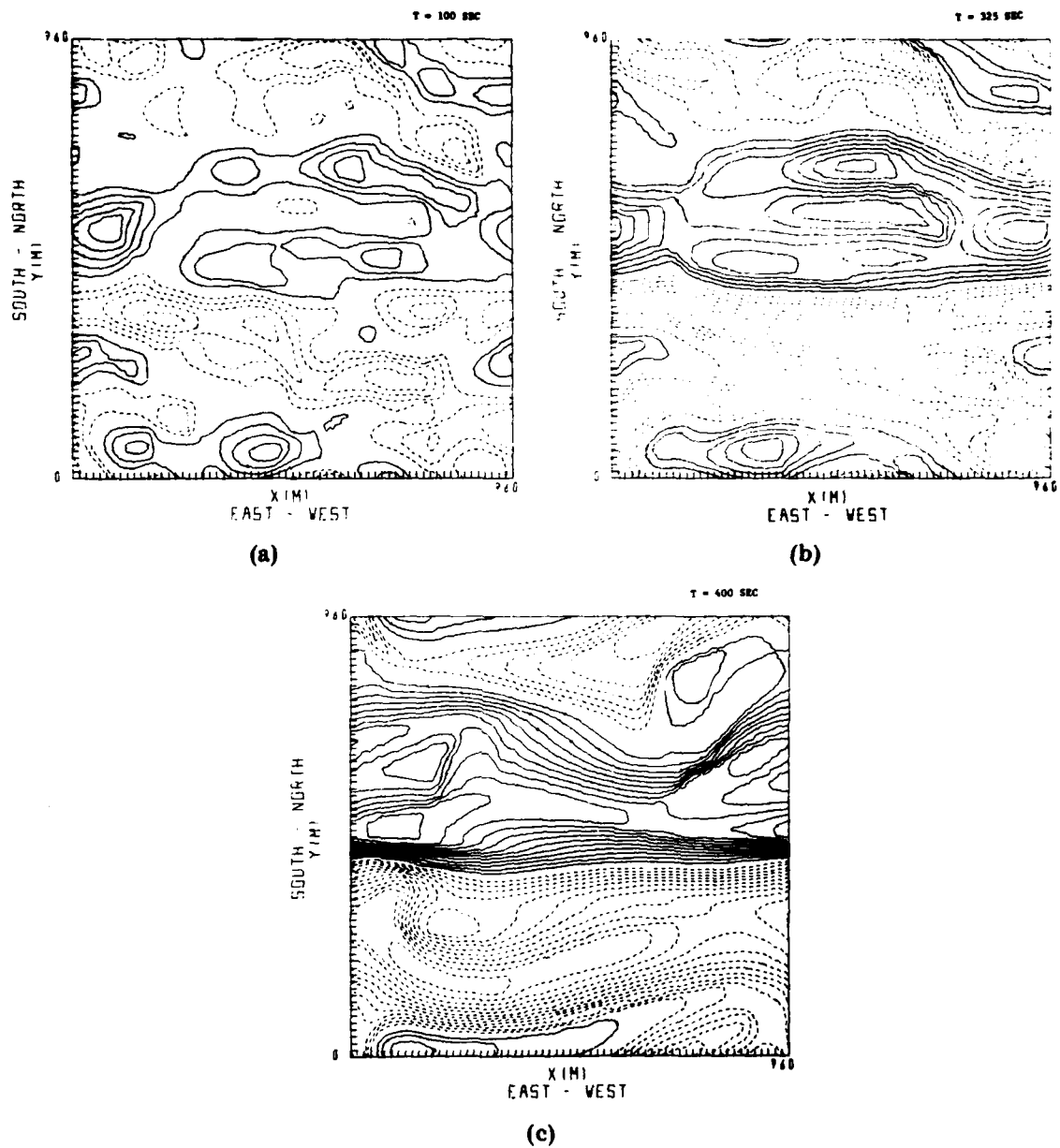
15

(a)

(b)

(c)

Fig. 5 — Isodensity contours of $\delta n/n_o$ for L = 5 km at (a) t = 100 sec, (b) t = 325 sec, (c) t = 400 sec for secondary, two-step process.

16

power spectra of these density irregularities are similar to those found in Model 1. To be sure, this model is very crude. We present it only as a basic illustration of the two-step irregularity generation mechanism. More realistic models will be studied in a future paper.

5. SUMMARY AND DISCUSSION

We have performed analytical and numerical simulation studies of small scale (0.1–1 km) irregularities in local unstable regions of large scale convecting plasma enhancements in the diffuse auroral F region ionosphere. We have shown that small scale size density fluctuations can be destabilized primarily on the poleward sides of equatorward convecting plasma slabs by a combination of the effects of convection and field aligned currents. In a plane nearly perpendicular to the magnetic field these simulations indicate that this destabilization leads to steepened striation-like structures (elongated in the north-south direction for equatorward convection) which can form and cascade from kilometer to tens of meter scale sizes on the order of an hour. The one-dimensional spatial power spectra of the density irregularities in the north-south $P(k_y) \propto k_y^{-n}$ and east-west $P(k_x)$ $\propto k_x^{-n}$ directions can be described by power laws with $n \simeq 2$–3 for wavelengths $2\pi/k_x$, $2\pi/k_y \simeq 80$–960 m. In addition, we show, using a very simple model, that the experimentally observed L-shell (east-west) aligned nature of small scale ($\lesssim 1$ km) irregularities in equatorward convecting large scale plasma enhancements might arise from a secondary, two-step process. In this theory, nonlinear long wavelength (~ 100 km) primary striations can create sharp east-west density gradients on which shorter scale size (< 1 km) irregularities can grow if the north-south electric field is of sufficient magnitude compared to the east-west field.

In this study we have examined the quasi two-dimensional linear and nonlinear evolution of small scale size (0.1–1km) irregularities in local unstable regions of larger scale (several hundreds of kilometers) convecting plasma enhancements in the diffuse auroral F region ionosphere. This has been accomplished by solving the plasma fluid equations in a horizontal plane approximately perpendicular to the magnetic field. The observed plasma enhancements are three dimensional [Vickrey et al., 1980]. However, the

horizontal gradients are much steeper than the vertical density gradients allowing one to approximately model the plasma enhancements by vertical slabs. In addition, we have not included a full spectrum of finite $k_\parallel$ modes in these simulations. However, since the modes with maximum linear growth rate have $k_\parallel/k_\perp \ll 1$, the important structuring processes will occur in the plane nearly perpendicular to the magnetic field.

Finally, we note that we have not addressed other related topics, e.g., the source mechanism of the plasma enhancements and their coupling to the E-region. These topics will be discussed in future studies.

ACKNOWLEDGMENTS

REFERENCES

Banks, P.M. and G. Kockarts, Aeronomy Part A (Academic Press, Inc., New York, NY, 1973).

Banks, P.M. and J.R. Doupnik, A review of auroral zone electrodynamics deduced from incoherent scatter observations, J. Atmos. Terr. Phys., 37, 951, 1975.

Chaturvedi, P.K. and S.L. Ossakow, Nonlinear stabilization of the current convective instability in the diffuse aurora, Geophys. Res. Lett., 6, 957, 1979.

Erukhimov, L.M., A.M. Lerner, V.I. Kosolapenko, and E.N. Myasnikov, The spectral form of small-scale plasma turbulence in the auroral ionosphere, Planet. Space Sci., 29, 931, 1981.

Fremouw, E.J., C.L. Rino, R.C. Livingston, and M.C. Cousins, A persistent subauroral scintillation enhancement observed in Alaska, Geophys. Res. Lett., 4, 539, 1977.

Hanuise, C., J.P. Villain, and M. Crochet, Spectral studies of F region irregularities in the auroral zone, Geophys. Res. Lett., 8, 1083, 1981.

Kadomtsev, B.B. and A.V. Nedospasov, Instability of the positive column in a magnetic field and the "anomalous diffusion effect," J. Nucl. Energy, Part C, 1, 230, 1960.

Kelley, M.C., K.D. Baker, J.C. Ulwick, C.L. Rino, and M.J. Baron, Simultaneous rocket probe, scintillation, and incoherent scatter radar observations of irregularities in the auroral zone ionosphere, Radio Sci., 15, 491, 1980.

Kelley, M.C. J.F. Vickrey, C.W. Carlson, and R. Torbert, On the origin and spatial extent of high-latitude F-region irregularities, J. Geophys. Res., (in press) 1982.

Keskinen, M.J., S.L. Ossakow, and B.E. McDonald, Nonlinear evolution of diffuse auroral F region ionospheric irregularities, Geophys. Res. Lett., 7, 573, 1980.

Keskinen, M.J. and S.L. Ossakow, Nonlinear evolution of plasma enhancements in the auroral ionosphere I: long wavelength irregularities, J. Geophys. Res., 87, 144, 1982.

Lee, W.W. and H. Okuda, Anomalous transport and stabilization of collisionless drift-wave instabilities, Phys. Rev. Lett., 36, 870, 1976.

19

Lehnert, B., Diffusion processes in the positive column in a longitudinal magnetic field, in Proceedings of the Second Geneva Conference on the Peaceful Uses of Atomic Energy, 32, 349, 1958.

Linson, L.M. and J.B. Workman, Formation of striations in ionospheric plasma clouds, J. Geophys. Res., 75, 3211, 1970.

Matsuda, Y. and H. Okuda, Simulation of dissipative trapped-electron instability in linear geometry, Phys. Rev. Lett., 36, 474, 1976.

McDonald, B.E., The Chebychev method for solving nonself-adjoint elliptic equations on vector computer, J. Comp. Phys., 35, 147, 1980.

Ossakow, S.L. and P.K. Chaturvedi, Current convective instability in the diffuse aurora, Geophys. Res. Lett., 6, 332, 1979.

Perkins, F.W. and J.H. Doles III, Velocity shear and the $E \times B$ instability, J. Geophys. Res., 80, 211, 1975.

Rino, C.L., R.C. Livingston, and S.J. Matthews, Evidence for sheet-like auroral ionospheric irregularities, Geophys. Res. Letts., 5, 1039, 1978.

Rino, C.L. and S.J. Matthews, On the morphology of auroral-zone radiowave scintillation, J. Geophys. Res., 85, 4139, 1980.

Rino, C.L. and J. Owen, The structure of localized nighttime auroral-zone scintillation enhancements, J. Geophys. Res., 85, 2941, 1980.

Rognlien, T.D. and J. Weinstock, Theory of the nonlinear spectrum of the gradient drift instability in the equatorial electrojet, J. Geophys. Res., 79, 4733, 1974.

Scannapieco, A.J., S.L. Ossakow, S.R. Goldman, and J.M. Pierre, Plasma cloud late time striation spectra, J. Geophys. Res., 81, 6037, 1976.

Schunk, R.W. and J.C.G. Walker, Theoretical ion densities in the lower atmosphere, Planet. Space Sci., 21, 1975, 1973.

Simon, A., Instability of a partially ionized plasma in crossed electric and magnetic fields, Phys. Fluids, 6, 382, 1963.

Vickrey, J.F., C.L. Rino, and T.A. Potemra, Chatanika/Triad observations of unstable ionization enhancements in the auroral F-region, Geophys. Res. Lett., 789, 1980.

Zabusky, N.J., J.H. Doles III, and F.W. Perkins, Deformation and striation of plasma clouds in the ionosphere, 2, Numerical simulation of a nonlinear two-dimensional model, J. Geophys. Res., 78, 711, 1973.

Zalesak, S.T., Fully multidimensional flux-corrected transport algorithms for fluids, J. Comp. Phys., 31, 335, 1979.

DISTRIBUTION LIST

DIRECTOR
BMD ADVANCED TECH CTR
HUNTSVILLE OFFICE
P.O. BOX 1500
HUNTSVILLE, AL 35807
  01CY ATTN ATC-T MELVIN T. CAPPS
  01CY ATTN ATC-O W. DAVIES
  01CY ATTN ATC-R DON RUSS

PROGRAM MANAGER
BMD PROGRAM OFFICE
5001 EISENHOWER AVENUE
ALEXANDRIA, VA 22333
  01CY ATTN DACS-BMT J. SHEA

CHIEF C-E- SERVICES DIVISION
U.S. ARMY COMMUNICATIONS CMD
PENTAGON RM 1B269
WASHINGTON, D.C. 20310
  01CY ATTN C- E-SERVICES DIVISION

COMMANDER
FRADCOM TECHNICAL SUPPORT ACTIVITY
DEPARTMENT OF THE ARMY
FORT MONMOUTH, N.J. 07703
  01CY ATTN DRSEL-NL-RD H. BENNET
  01CY ATTN DRSEL-PL-ENV H. BOMKE
  01CY ATTN J.E. QUIGLEY

COMMANDER
HARRY DIAMOND LABORATORIES
DEPARTMENT OF THE ARMY
2800 POWDER MILL ROAD
ADELPHI, MD 20783
  (CNWDI-INNER ENVELOPE: ATTN: DELHD-RBH)
  01CY ATTN DELHD-TI M. WEINER
  01CY ATTN DELHD-RB R. WILLIAMS
  01CY ATTN DELHD-NP F. WIMENITZ
  01CY ATTN DELHD-NP C. MOAZED

COMMANDER
U.S. ARMY COMM-ELEC ENGRG INSTAL AGY
FT. HUACHUCA, AZ 85613
  01CY ATTN CCC-EMEO GEORGE LANE

COMMANDER
U.S. ARMY FOREIGN SCIENCE & TECH CTR
220 7TH STREET, NE
CHARLOTTESVILLE, VA 22901
  01CY ATTN DRXST-SD
  01CY ATTN R. JONES

COMMANDER
U.S. ARMY MATERIAL DEV & READINESS CMD
5001 EISENHOWER AVENUE
ALEXANDRIA, VA 22333

  01CY ATTN DRCLDC J.A. BENDER
COMMANDER
U.S. ARMY NUCLEAR AND CHEMICAL AGENCY
7500 BACKLICK ROAD
BLDG 2073
SPRINGFIELD, VA 22150
  01CY ATTN LIBRARY

DIRECTOR
U.S. ARMY BALLISTIC RESEARCH LABORATORY
ABERDEEN PROVING GROUND, MD 21005
  01CY ATTN TECH LIBRARY EDWARD BAICY

COMMANDER
U.S. ARMY SATCOM AGENCY
FT. MONMOUTH, NJ 07703
  01CY ATTN DOCUMENT CONTROL

COMMANDER
U.S. ARMY MISSILE INTELLIGENCE AGENCY
REDSTONE ARSENAL, AL 35809
  01CY ATTN JIM GAMBLE

DIRECTOR
U.S. ARMY TRADOC SYSTEMS ANALYSIS ACTIVITY
WHITE SANDS MISSILE RANGE, NM 88002
  01CY ATTN ATAA-SA
  01CY ATTN TCC/F. PAYAN JR.
  01CY ATTN ATTA-TAC LTC J. HESSE

COMMANDER
NAVAL ELECTRONIC SYSTEMS COMMAND
WASHINGTON, D.C. 20360
  01CY ATTN NAVALEX 034 T. HUGHES
  01CY ATTN PME 117
  01CY ATTN PME 117-T
  01CY ATTN CODE 5011

COMMANDING OFFICER
NAVAL INTELLIGENCE SUPPORT CTR
4301 SUITLAND ROAD, BLDG. 5
WASHINGTON, D.C. 20390
  01CY ATTN MR. DUBBIN STIC 12
  01CY ATTN NISC-50
  01CY ATTN CODE 5404 J. GALET

COMMANDER
NAVAL OCCEAN SYSTEMS CENTER
SAN DIEGO, CA 92152
  03CY ATTN CODE 532 W. MOLER
  01CY ATTN CODE 0230 C. BAGGETT
  01CY ATTN CODE 81 R. EASTMAN

DIRECTOR
NAVAL RESEARCH LABORATORY
WASHINGTON, D.C. 20375
  01CY ATTN CODE 4700 S. L. Ossakow
      26 CYS IF UNCLASS. 1 CY IF CLASS)
  01CY ATTN CODE 4701 JACK D. BROWN
  01CY ATTN CODE 4780 BRANCH HEAD (150
      CYS IF UNCLASS, 1 CY IF CLASS)
  01CY ATTN CODE 7500
  01CY ATTN CODE 7550
  01CY ATTN CODE 7580
  01CY ATTN CODE 7551
  01CY ATTN CODE 7555
  01CY ATTN CODE 4730 E. MCLEAN
  01CY ATTN CODE 4187
  20CY ATTN CODE 2628

COMMANDER
NAVAL SEA SYSTEMS COMMAND
WASHINGTON, D.C. 20362
  01CY ATTN CAPT R. PITKIN

COMMANDER
NAVAL SPACE SURVEILLANCE SYSTEM
DAHLGREN, VA 22448
  01CY ATTN CAPT J.H. BURTON

OFFICER-IN-CHARGE
NAVAL SURFACE WEAPONS CENTER
WHITE OAK, SILVER SPRING, MD 20910
  01CY ATTN CODE F31

DIRECTOR
STRATEGIC SYSTEMS PROJECT OFFICE
DEPARTMENT OF THE NAVY
WASHINGTON, D.C. 20376
  01CY ATTN NSP-2141
  01CY ATTN NSSP-2722 FRED WIMBERLY

COMMANDER
NAVAL SURFACE WEAPONS CENTER
DAHLGREN LABORATORY
DAHLGREN, VA 22448
  01CY ATTN CODE DF-14 R. BUTLER

OFFICE OF NAVAL RESEARCH
ARLINGTON, VA 22217
  01CY ATTN CODE 465
  01CY ATTN CODE 461
  01CY ATTN CODE 402
  01CY ATTN CODE 420
  01CY ATTN CODE 421

COMMANDER
AEROSPACE DEFENSE COMMAND/DC
DEPARTMENT OF THE AIR FORCE
ENT AFB, CO 80912
  01CY ATTN DC MR. LONG

COMMANDER
AEROSPACE DEFENSE COMMAND/XPD
DEPARTMENT OF THE AIR FORCE
ENT AFB, CO 80912
  01CY ATTN XPDQQ
  01CY ATTN XP

AIR FORCE GEOPHYSICS LABORATORY
HANSCOM AFB, MA 01731
  01CY ATTN OPR HAROLD GARDNER
  01CY ATTN LKB KENNETH S.W. CHAMPION
  01CY ATTN OPR ALVA T. STAIR
  01CY ATTN PHP JULES AARONS
  01CY ATTN PHD JURGEN BUCHAU
  01CY ATTN PHI JOHN P. MULLEN

AF WEAPONS LABORATORY
KIRTLAND AFT, NM 87117
  01CY ATTN SUL
  01CY ATTN CA ARTHUR H. GUENTHER
  01CY ATTN NTYCE 1LT. G. KRAJEI

AFTAC
PATRICK AFB, FL 32925
  01CY ATTN TF/MAJ WILEY
  01CY ATTN TN

AIR FORCE AVIONICS LABORATORY
WRIGHT-PATTERSON AFB, OH 45433
  01CY ATTN AAD WADE HUNT
  01CY ATTN AAD ALLEN JOHNSON

DEPUTY CHIEF OF STAFF
RESEARCH, DEVELOPMENT, & ACQ
DEPARTMENT OF THE AIR FORCE
WASHINGTON, D.C. 20330
  01CY ATTN AFRDQ

HEADQUATERS
ELECTRONIC SYSTEMS DIVISION/XR
DEPARTMENT OF THE AIR FORCE
HANSCOM AFB, MA 01731
  01CY ATTN XR J. DEAS

HEADQUATERS
ELECTRONIC SYSTEMS DIVISION/YSEA
DEPARTMENT OF THE AIR FORCE
HANSCOM AFB, MA 01732
  01CY ATTN YSEA

HEADQUATERS
ELECTRONIC SYSTEMS DIVISION/DC
DEPARTMENT OF THE AIR FORCE
HANSCOM AFB, MA 01731
  01CY ATTN DCKC MAJ J.C. CLARK

COMMANDER
FOREIGN TECHNOLOGY DIVISION, AFSC
WRIGHT-PATTERSON AFB, OH 45433
    01CY ATTN NICD LIBRARY
    01CY ATTN ETDP B. BALLARD

COMMANDER
ROME AIR DEVELOPMENT CENTER, AFSC
GRIFFISS AFB, NY 13441
    01CY ATTN DOC LIBRARY/TSLD
    01CY ATTN OCSE V. COYNE

SAMSO/SZ
POST OFFICE BOX 92960
WORLDWAY POSTAL CENTER
LOS ANGELES, CA 90009
    (SPACE DEFENSE SYSTEMS)
    01CY ATTN SZJ

STRATEGIC AIR COMMAND/XPFS
OFFUTT AFB, NE 68113
    01CY ATTN XPFS MAJ B. STEPHAN
    01CY ATTN ADWATE MAJ BRUCE BAUER
    01CY ATTN NRT
    01CY ATTN DOK CHIEF SCIENTIST

SAMSO/SK
P.O. BOX 92960
WORLDWAY POSTAL CENTER
LOS ANGELES, CA 90009
    01CY ATTN SKA (SPACE COMM SYSTEMS)
        M. CLAVIN

SAMSO/MN
NORTON AFB, CA 92409
(MINUTEMAN)
    01CY ATTN MNNL LTC KENNEDY

COMMANDER
ROME AIR DEVELOPMENT CENTER, AFSC
HANSCOM AFB, MA 01731
    01CY ATTN EEP A. LORENTZEN

DEPARTMENT OF ENERGY
LIBRARY ROOM G-042
WASHINGTON, D.C. 20545
    01CY ATTN DOC CON FOR A. LABOWITZ

DEPARTMENT OF ENERGY
ALBUQUERQUE OPERATIONS OFFICE
P.O. BOX 5400
ALBUQUERQUE, NM 87115
    01CY ATTN DOC CON FOR D. SHERWOOD

EG&G, INC.
LOS ALAMOS DIVISION
P.O. BOX 809
LOS ALAMOS, NM 85544
    01CY ATTN DOC CON FOR J. BREEDLOVE

UNIVERSITY OF CALIFORNIA
LAWRENCE LIVERMORE LABORATORY
P.O. BOX 808
LIVERMORE, CA 94550
    01CY ATTN DOC CON FOR TECH INFO DEPT
    01CY ATTN DOC CON FOR L-389 R. OTT
    01CY ATTN DOC CON FOR L-31 R. HAGER
    01CY ATTN DOC CON FOR L-46 F. SEWARD

LOS ALAMOS NATIONAL LABORATORY
P.O. BOX 1663
LOS ALAMOS, NM 87545
    01CY ATTN DOC CON FOR J. WOLCOTT
    01CY ATTN DOC CON FOR R.F. TASCHEK
    01CY ATTN DOC CON FOR E. JONES
    01CY ATTN DOC CON FOR J. MALIK
    01CY ATTN DOC CON FOR R. JEFFRIES
    01CY ATTN DOC CON FOR J. ZINN
    01CY ATTN DOC CON FOR P. KEATON
    01CY ATTN DOC CON FOR E. WESTERVELT

SANDIA LABORATORIES
P.O. BOX 5800
ALBUQUERQUE, NM 87115
    01CY ATTN DOC CON FOR W. BROWN
    01CY ATTN DOC CON FOR A. THORNBROUGH
    01CY ATTN DOC CON FOR T. WRIGHT
    01CY ATTN DOC CON FOR D. DAHLGREN
    01CY ATTN DOC CON FOR 3141
    01CY ATTN DOC CON FOR SPACE PROJECT DIV

SANDIA LABORATORIES
LIVERMORE LABORATORY
P.O. BOX 969
LIVERMORE, CA 94550
    01CY ATTN DOC CON FOR B. MURPHEY
    01CY ATTN DOC CON FOR T. COOK

OFFICE OF MILITARY APPLICATION
DEPARTMENT OF ENERGY
WASHINGTON, D.C. 20545
    01CY ATTN DOC CON DR. YO SONG

OTHER GOVERNMENT

DEPARTMENT OF COMMERCE
NATIONAL BUREAU OF STANDARDS
WASHINGTON, D.C. 20234
    (ALL CORRES: ATTN SEC OFFICER FOR)
    01CY ATTN R. MOORE

24

INSTITUTE FOR TELECOM SCIENCES
NATIONAL TELECOMMUNICATIONS & INFO ADMIN
BOULDER, CO 80303
    01CY ATTN A. JEAN (UNCLASS ONLY)
    01CY ATTN W. UTLAUT
    01CY ATTN D. CROMBIE
    01CY ATTN L. BERRY

NATIONAL OCEANIC & ATMOSPHERIC ADMIN
ENVIRONMENTAL RESEARCH LABORATORIES
DEPARTMENT OF COMMERCE
BOULDER, CO 80302
    01CY ATTN R. GRUBB
    01CY ATTN AERONOMY LAB G. REID

DEPARTMENT OF DEFENSE CONTRACTORS

AEROSPACE CORPORATION
P.O. BOX 92957
LOS ANGELES, CA 90009
    01CY ATTN I. GARFUNKEL
    01CY ATTN T. SALMI
    01CY ATTN V. JOSEPHSON
    01CY ATTN S. BOWER
    01CY ATTN N. STOCKWELL
    01CY ATTN D. OLSEN

ANALYTICAL SYSTEMS ENGINEERING CORP
5 OLD CONCORD ROAD
BURLINGTON, MA 01803
    01CY ATTN RADIO SCIENCES

BERKELEY RESEARCH ASSOCIATES, INC.
P.O. BOX 983
BERKELEY, CA 94701
    01CY ATTN J. WORKMAN
    01CY ATTN C. PRETTIE

BOEING COMPANY, THE
P.O. BOX 3707
SEATTLE, WA 98124
    01CY ATTN G. KEISTER
    01CY ATTN D. MURRAY
    01CY ATTN G. HALL
    01CY ATTN J. KENNEY

BROWN ENGINEERING COMPANY, INC.
CUMMINGS RESEARCH PARK
HUNTSVILLE, AL 35807
    01CY ATTN ROMEO A. DELIBERIS

CALIFORNIA AT SAN DIEGO, UNIV OF
P.O. BOX 6049
SAN DIEGO, CA 92106

CHARLES STARK DRAPER LABORATORY, INC.
555 TECHNOLOGY SQUARE
CAMBRIDGE, MA 02139
    01CY ATTN D.B. COX
    01CY ATTN J.P. GILMORE

COMSAT LABORATORIES
LINTHICUM ROAD
CLARKSBURG, MD 20734
    01CY ATTN G. HYDE

CORNELL UNIVERSITY
DEPARTMENT OF ELECTRICAL ENGINEERING
ITHACA, NY 14850
    01CY ATTN D.T. FARLEY, JR.

ELECTROSPACE SYSTEMS, INC.
BOX 1359
RICHARDSON, TX 75080
    01CY ATTN H. LOGSTON
    01CY ATTN SECURITY (PAUL PHILLIPS)

ESL, INC.
495 JAVA DRIVE
SUNNYVALE, CA 94086
    01CY ATTN J. ROBERTS
    01CY ATTN JAMES MARSHALL

GENERAL ELECTRIC COMPANY
SPACE DIVISION
VALLEY FORGE SPACE CENTER
GODDARD BLVD KING OF PRUSSIA
P.O. BOX 8555
PHILADELPHIA, PA 19101
    01CY ATTN M.H. BORTNER SPACE SCI LAB

GENERAL ELECTRIC COMPANY
P.O. BOX 1122
SYRACUSE, NY 13201
    01CY ATTN F. REIBERT

GENERAL ELECTRIC TECH SERVICES CO., INC.
HMES
COURT STREET
SYRACUSE, NY 13201
    01CY ATTN G. MILLMAN

GENERAL RESEARCH CORPORATION
SANTA BARBARA DIVISION
P.O. BOX 6770
SANTA BARBARA, CA 93111
    01CY ATTN JOHN ISE, JR.
    01CY ATTN JOEL GARBARINO

GEOPHYSICAL INSTITUTE
UNIVERSITY OF ALASKA
FAIRBANKS, AK 99701
  (ALL CLASS ATTN: SECURITY OFFICER)
  01CY ATTN T.N. DAVIS (UNCLASS ONLY)
  01CY ATTN TECHNICAL LIBRARY
  01CY ATTN NEAL BROWN (UNCLASS ONLY)

GTE SYLVANIA, INC.
ELECTRONICS SYSTEMS GRP-EASTERN DIV
77 A STREET
NEEDHAM, MA 02194
  01CY ATTN MARSHALL CROSS

HSS, INC.
2 ALFRED CIRCLE
BEDFORD, MA 01730
  01CY ATTN DONALD HANSEN

ILLINOIS, UNIVERSITY OF
107 COBLE HALL
150 DAVENPORT HOUSE
CHAMPAIGN, IL 61820
  (ALL CORRES ATTN DAN MCCLELLAND)
  01CY ATTN K. YEH

INSTITUTE FOR DEFENSE ANALYSES
400 ARMY-NAVY DRIVE
ARLINGTON, VA 22202
  01CY ATTN J.M. AEIN
  01CY ATTN ERNEST BAUER
  01CY ATTN HANS WOLFARD
  01CY ATTN JOEL BENGSTON

INTL TEL & TELEGRAPH CORPORATION
500 WASHINGTON AVENUE
NUTLEY, NJ 07110
  01CY ATTN TECHNICAL LIBRARY

JAYCOR
11011 TORREYANA ROAD
P.O. BOX 85154
SAN DIEGO, CA 92138
  01CY ATTN J.L. SPERLING

JOHNS HOPKINS UNIVERSITY
APPLIED PHYSICS LABORATORY
JOHNS HOPKINS ROAD
LAUREL, MD 20810
  01CY ATTN DOCUMENT LIBRARIAN
  01CY ATTN THOMAS POTEMRA
  01CY ATTN JOHN DASSOULAS

KAMAN SCIENCES CORP
P.O. BOX 7463
COLORADO SPRINGS, CO 80933

  01CY ATTN T. MEAGHER
KAMAN TEMPO-CENTER FOR ADVANCED STUDIES
816 STATE STREET (P.O DRAWER QQ)
SANTA BARBARA, CA 93102
  01CY ATTN DASIAC
  01CY ATTN TIM STEPHANS
  01CY ATTN WARREN S. KNAPP
  01CY ATTN WILLIAM MCNAMARA
  01CY ATTN B. GAMBILL

LINKABIT CORP
10453 ROSELLE
SAN DIEGO, CA 92121
  01CY ATTN IRWIN JACOBS

LOCKHEED MISSILES & SPACE CO., INC
P.O. BOX 504
SUNNYVALE, CA 94088
  01CY ATTN DEPT 60-12
  01CY ATTN D.R. CHURCHILL

LOCKHEED MISSILES & SPACE CO., INC.
3251 HANOVER STREET
PALO ALTO, CA 94304
  01CY ATTN MARTIN WALT DEPT 52-12
  01CY ATTN W.L. IMHOF DEPT 52-12
  01CY ATTN RICHARD G. JOHNSON DEPT 52-12
  01CY ATTN J.B. CLADIS DEPT 52-12

LOCKHEED MISSILE & SPACE CO., INC.
HUNTSVILLE RESEARCH & ENGR. CTR.
4800 BRADFORD DRIVE
HUNTSVILLE, AL 35807
  ATTN DALE H. DIVIS

MARTIN MARIETTA CORP
ORLANDO DIVISION
P.O. BOX 5837
ORLANDO, FL 32805
  01CY ATTN R. HEFFNER

M.I.T. LINCOLN LABORATORY
P.O. BOX 73
LEXINGTON, MA 02173
  01CY ATTN DAVID M. TOWLE
  01CY ATTN P. WALDRON
  01CY ATTN L. LOUGHLIN
  01CY ATTN D. CLARK

MCDONNEL DOUGLAS CORPORATION
5301 BOLSA AVENUE
HUNTINGTON BEACH, CA 92647
  01CY ATTN N. HARRIS
  01CY ATTN J. MOULE
  01CY ATTN GEORGE MROZ
  01CY ATTN W. OLSON
  01CY ATTN R.W. HALPRIN

SRI INTERNATIONAL
333 RAVENSWOOD AVENUE
MENLO PARK, CA 94025
  01CY ATTN DONALD NEILSON
  01CY ATTN ALAN BURNS
  01CY ATTN G. SMITH
  01CY ATTN L.L. COBB
  01CY ATTN DAVID A. JOHNSON
  01CY ATTN WALTER G. CHESNUT
  01CY ATTN CHARLES L. RINO
  01CY ATTN WALTER JAYE
  01CY ATTN M. BARON
  01CY ATTN RAY L. LEADABRAND
  01CY ATTN G. CARPENTER
  01CY ATTN G. PRICE
  01CY ATTN J. PETERSON
  01CY ATTN R. HAKE, JR.
  01CY ATTN V. GONZALES
  01CY ATTN D. MCDANIEL

STEWART RADIANCE LABORATORY
UTAH STATE UNIVERSITY
1 DE ANGELO DRIVE
BEDFORD, MA 01730
  01CY ATTN J. ULWICK

TECHNOLOGY INTERNATIONAL CORP
75 WIGGINS AVENUE
BEDFORD, MA 01730
  01CY ATTN W.P. BOQUIST

TRW DEFENSE & SPACE SYS GROUP
ONE SPACE PARK
REDONDO BEACH, CA 90278
  01CY ATTN R. K. PLEBUCH
  01CY ATTN S. ALTSCHULER
  01CY ATTN D. DEE

VISIDYNE
SOUTH BEDFORD STREET
BURLINGTON, MASS 01803
  01CY ATTN W. REIDY
  01CY ATTN J. CARPENTER
  01CY ATTN C. HUMPHREY

IONOSPHERIC MODELING DISTRIBUTION LIST
(UNCLASSIFIED ONLY)

PLEASE DISTRIBUTE ONE COPY TO EACH OF THE FOLLOWING PEOPLE:

NAVAL RESEARCH LABORATORY
WASHINGTON, D.C. 20375
  DR. P. MANGE - CODE 4101
  DR. R. MEIER - CODE 4141
  DR. E. SZUSZCZEWICZ - CODE 4187
  DR. J. GOODMAN - CODE 4180
  Dr. R. RODRIGUEZ - CODE 4187

A.F. GEOPHYSICS LABORATORY
L.G. HANSCOM FIELD
BEDFORD, MA 01730
  DR. T. ELKINS
  DR. W. SWIDER
  MRS. R. SAGALYN
  DR. J.M. FORBES
  DR. T.J. KENESHEA
  DR. J. AARONS
  DR. H. CARLSON
  DR. J. JASPERSE

CORNELL UNIVERSITY
ITHACA, NY 14850
  DR. W.E. SWARTZ
  DR. R. SUDAN
  DR. D. FARLEY
  DR. M. KELLEY

HARVARD UNIVERSITY
HARVARD SQUARE
CAMBRIDGE, MA 02138
  DR. M.B. McELROY
  DR. R. LINDZEN

INSTITUTE FOR DEFENSE ANALYSIS
400 ARMY/NAVY DRIVE
ARLINGTON, VA 22202
  DR. E. BAUER

MASSACHUSETTS INSTITUTE OF TECHNOLOGY
PLASMA FUSION CENTER
LIBRARY, NW16-262
CAMBRIDGE, MA 02139

NASA
GODDARD SPACE FLIGHT CENTER
GREENBELT, MD 20771
  DR. S. CHANDRA
  DR. K. MAEDA
  DR. R.F. BENSON

NATIONAL TECHNICAL INFORMATION CENTER
CAMERON STATION
ALEXANDRIA, VA 22314
  12CY ATTN TC

COMMANDER
NAVAL AIR SYSTEMS COMMAND
DEPARTMENT OF THE NAVY
WASHINGTON, D.C. 20360
  DR. T. CZUBA

COMMANDER
NAVAL OCEAN SYSTEMS CENTER
SAN DIEGO, CA 92152
  MR. R. ROSE - CODE 5321

NOAA
DIRECTOR OF SPACE AND ENVIRONMENTAL
    LABORATORY
BOULDER, CO 80302
  DR. A. GLENN JEAN
  DR. G.W. ADAMS
  DR. D.N. ANDERSON
  DR. K. DAVIES
  DR. R. F. DONNELLY

OFFICE OF NAVAL RESEARCH
800 NORTH QUINCY STREET
ARLINGTON, VA 22217
  DR. H. MULLANEY

PENNSYLVANIA STATE UNIVERSITY
UNIVERSITY PARK, PA 16802
  DR. J.S. NISBET
  DR. P.R. ROHRBAUGH
  DR. L.A. CARPENTER
  DR. M. LEE
  DR. R. DIVANY
  DR. P. BENNETT
  DR. E. KLEVANS

PRINCETON UNIVERSITY
PLASMA PHYSICS LABORATORY
PRINCETON, NJ 08540
  DR. F. PERKINS

29

SCIENCE APPLICATIONS, INC.
1150 PROSPECT PLAZA
LA JOLLA, CA 92037
   DR. D.A. HAMLIN
   DR. L. LINSON
   DR. E. FRIEMAN

STANFORD UNIVERSITY
STANFORD, CA 94305
   DR. P.M. BANKS

U.S. ARMY ABERDEEN RESEARCH
   AND DEVELOPMENT CENTER
BALLISTIC RESEARCH LABORATORY
ABERDEEN, MD
   DR. J. HEIMERL

UNIVERSITY OF CALIFORNIA,
   BERKELEY
BERKELEY, CA 94720
   DR. M. HUDSON

UNIVERSITY OF CALIFORNIA
LOS ALAMOS SCIENTIFIC LABORATORY
J-10, MS-664
LOS ALAMOS, NM 87545
   M. PONGRATZ
   D. SIMONS
   G. BARASCH
   L. DUNCAN
   P. BERNHARDT

UNIVERSITY OF CALIFORNIA,
   LOS ANGELES
405 HILLGARD AVENUE
LOS ANGELES, CA 90024
   DR. F.V. CORONITI
   DR. C. KENNEL
   DR. A.Y. WONG

UNIVERSITY OF MARYLAND
COLLEGE PARK, MD 20740
   DR. K. PAPADOPOULOS
   DR. E. OTT

UNIVERSITY OF PITTSBURGH
PITTSBURGH, PA 15213
   DR. N. ZABUSKY
   DR. M. BIONDI
   DR. E. OVERMAN

UTAH STATE UNIVERSITY
4TH AND 8TH STREETS
LOGAN, UTAH 84322
   DR. R. HARRIS
   DR. K. BAKER
   DR. R. SCHUNK

DATE
ILME
_8